Available online at www.sciencedirect.com
SCIENCE DIRECT®
Journal of Power Sources 118 (2003) 286–297
JOURNAL OF POWER SOURCES
www.elsevier.com/locate/jpowsour

Mixture preparation by cool flames for diesel-reforming technologies

L. Hartmann*, K. Lucka, H. Köhne

Oel-Wärme-Institut gGmbH, Kaiserstraße 100, D-52134 Herzogenrath, Germany

Abstract

The separation of the evaporation from the high-temperature reaction zone is crucial for the reforming process. Unfavorable mixtures of liquid fuels, water and air lead to degradation by local hot spots in the sensitive catalysts and formation of unwanted by-products in the reformer. Furthermore, the evaporator has to work with dynamic changes in the heat transfer, residence times and educt compositions. By using exothermal pre-reactions in the form of cool flames it is possible to realize a complete and residue-free evaporation of liquid hydrocarbon mixtures. The conditions whether cool flames can be stabilised or not is related to the heat release of the pre-reactions in comparison to the heat losses of the system.

Examinations were conducted in a flow reactor at atmospheric pressure and changing residence times to investigate the conditions under which stable cool flame operation is possible and auto-ignition or quenching occurs. An energy balance of the evaporator should deliver the values of heat release by cool flames in comparison to the heat losses of the system.

The cool flame evaporation is applied in the design of several diesel-reforming processes (thermal and catalytic partial oxidation, autothermal reforming) with different demands in the heat management and operation range (air ratio λ, steam-to-carbon ratio, SCR). The results are discussed at the end of this paper.

Keywords: Partial oxidation; Autothermal reforming; Cool flame; Mixture preparation; Diesel fuel; Fuel cell

1. Introduction

The mixture generation constitutes a key factor in terms of the quality of a reforming reaction. If the components of this mixture are not homogeneous, the tendency for soot to be formed or hot spots in the sensitive catalysts will increase. To prevent such inhomogeneties, efforts are made to establish a homogenous fuel/air/water mixture prior to the high-temperature oxidation zone. Therefore, liquid fuels, such as diesel, first have to be atomised and vaporised into microscopically sized droplets. Temperatures of 400 °C, however, are required for the evaporation, since the upper boiling point of diesel and industrial gas oil (IGO) lies at around 380 °C. With direct vaporisation into a pre-heated air stream the vaporisation can be provided by saturation. In Fig. 1, the calculated saturation temperatures for selected *n*-alkanes are given in respect to the air ratio λ. Relating to diesel or IGO an exact saturation temperature cannot be affected, since these fuels are composed of hundreds of different hydrocarbon species. To appreciate the necessary evaporation temperature for diesel or IGO as a C13 hydrocarbon, the saturation curve of pentadecane should be sufficient. According to this, a temperature of 150–170 °C is sufficient for the saturation in air under reformer conditions and an infinite time scale.

Commonly, the evaporation takes place in temperature areas and under residence times where auto-ignition can occur. Fig. 2 gives the ignition temperatures under atmospheric conditions in a flow reactor for industrial gas oil, which is based on nearly the same composition as diesel.

One model to describe the ignition process is the thermal ignition model, in which an auto-ignition arises from the self-heating produced by exothermic low-temperature reactions. The question whether it comes to an explosion or not is related to the heat release in comparison to the heat losses of the system. Generally, the heat release $\dot{R}$ (Eq. (1)) rises exponentially with the temperature governed by the Arrhenius equation whereas the heat losses $\dot{L}$ (Eq. (2)) can be described by linear temperature behaviour due to the Newton law of cooling. The impellent temperature difference is given by the mixture temperature T and the wall temperature T_W.

$$\dot{R} = \frac{\dot{Q}_r}{V} = \Delta U A^* \, e^{(-E/(R_n T))} c_f \quad (1)$$

$$\dot{L} = \frac{\dot{Q}_l}{V} = \alpha \frac{A}{V} (T - T_W) \quad (2)$$

* Corresponding author.
E-mail address: l.hartmann@owi-aachen.de (L. Hartmann).

0378-7753/03/$ – see front matter © 2003 Elsevier Science B.V. All rights reserved.
doi:10.1016/S0378-7753(03)00100-9

Nomenclature

A^*	pre-exponential factor
A	surface
$\dot{B}$	volume-based balance heat supply
c	concentration
c_p	specific heat capacity
d	diameter
E	activation energy
$\dot{H}$	enthalpy flow
$\dot{L}$	volume-based heat loss
$\dot{m}$	mass flow
$\dot{n}$	mole flow
p	pressure
P	power
r	recirculation ratio
R_n	universal gas constant
$\dot{R}$	volume-based heat release
$\dot{Q}$	heat flow
$\dot{Q}_r$	heat release flow
SV	space velocity
T	temperature
T_{init}	initial temperature
T_s	stable temperature
T_W	wall temperature
V	volume
Greek letters	
λ	air ratio
ϑ	temperature
τ_R	residence time
ϑ_{air}	air pre-heating temperature
ϑ_{educts}	educt temperature
η_{ref}	reforming efficiency
$\Delta\dot{H}$	enthalpy flow difference
ΔT	temperature difference
ΔU	difference of internal energy

In a certain temperature range a divergence from the Arrhenius behaviour can be observed for several fuels including diesel or IGO. This temperature region is characterised by a decrease of the heat release with an increase of the temperature. It is also referred as the negative temperature coefficient (NTC). The key to this characteristic lies in the lack of stability of the links formed within the chain reactions as a result of oxygen being absorbed.

Fig. 3 shows the relationship between the heat release and the heat losses in a closed vessel at different fixed surface temperatures for a mixture with NTC characteristic. If the temperature of the mixture is below the initialisation temperature T_{init}, the heat losses dominate the heat production. No relevant pre-reactions can be observed in the mixture. If the temperature exceeds the value of T_{init}, which has been identified for IGO in a range of 300 °C, the heat production tops the heat losses and a temperature increase up to $\Delta T = 180$ K is noticeable. As long as there is an intersection between $\dot{R}$ and $\dot{L}$ stable conditions could be established. The system will remain at a stationary state with constant temperature T_s. If the temperature is changed somewhat the system will return back to the stable point. This form of low-temperature reaction is called cool flame.

Within this paper the cool flames have been investigated to realise a complete and residue-free evaporation of liquid hydrocarbon mixtures. The target is to determine the limits of cool flame stability in respect to three different fuel processor boundary conditions:

- thermal partial oxidation (TPOX);
- catalytic partial oxidation (CPO);
- autothermal reforming (ATR).

2. Experimental

2.1. Cool flame evaporation

The cool flame experiments are conducted in stainless steel tubes with diameters between 50 and 100 mm. The total length of the cool flame reactor is 200 mm in principle. The tube is contained in an insulation tube equipped with an electrical radiation heating.

The air is pre-heated with a heating cartridge up to 650 °C. The air flow is controlled by mass flow controller. The fuel (industrial gas oil) is supplied to an injector with ambient temperature and injected via commercially available simplex pressure atomizer (0.4 gal/h, 60°S LE) pulsating with 50 Hz. The power output is determined gravimetrically. The axially mounted fuel injector is water cooled to keep the nozzle temperature below 120 °C.

The initialisation of the cool flame reactions takes place when the hydrocarbons are atomised in the pre-heated evaporator. For a technical evaporator, the heat needed to actuate the pre-reaction can be produced with a start-up burner. Once the cool flame has been initialised, air pre-heating is not mandatory when the hot product gas of the cool flame is re-circulated into the reaction zone by aerodynamic methods.

All heat fluxes and flows of enthalpies have been measured to draw an energy balance of the evaporator tube. The existing energy flows in the setup are given in Fig. 4.

For simplification, the assumption was considered that the outlet product gas consists only of air and oil vapour. Thus, the enthalpy flow of the product gas can be described as follows:

$$\dot{H}_{product} = \dot{H}_{air,out} + \dot{H}_{f,out} \quad (3)$$

The heat release of the cool flame reaction $\dot{Q}_r$ is calculated by the balance heat supply of the evaporator tube

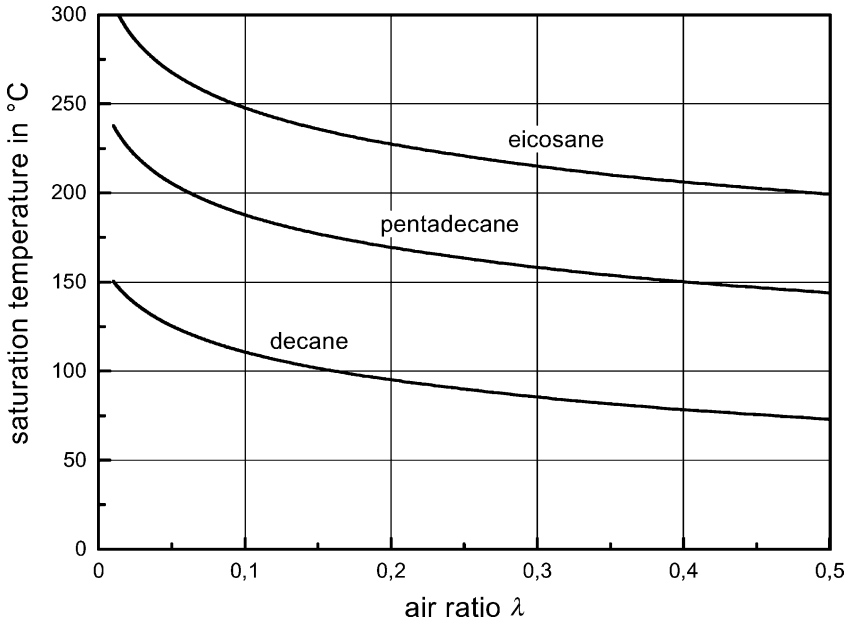

Fig. 1. Saturation temperatures of *n*-alkanes in respect to the air ratio λ [1].

$\dot{Q}$ and the differences of the enthalpy flows of air $\Delta\dot{H}_{\text{air}}$ and fuel $\Delta\dot{H}_{\text{f}}$.

$$\dot{Q} + \dot{Q}_{\text{r}} = \Delta\dot{H}_{\text{air}} + \Delta\dot{H}_{\text{f}} \tag{4}$$

The balance heat supply $\dot{Q}$ is given by Eq. (5). It is assembled by the heat supply of the electric heaters and the heat losses of water cooling and insulation.

$$\dot{Q} = \underbrace{P_{\text{air pre-heating}} + P_{\text{heating}}}_{\text{heat supply}} - \underbrace{(\dot{Q}_{\text{cooling water}} + \dot{Q}_{\text{surface}})}_{\text{heat losses}} \tag{5}$$

The flows of enthalpy were calculated by the temperatures, the mass flows and the specific heat capacities c_p of fuel and air.

$$\Delta\dot{H}_{\text{air}} = \dot{m}_{\text{air}}[c_{p,\text{air}}]_{\vartheta_{\text{in}}}^{\vartheta_{\text{out}}}(\vartheta_{\text{out}} - \vartheta_{\text{in}}) \tag{6}$$

$$\Delta\dot{H}_{\text{f}} = \dot{m}_{\text{f}}([c_{p,\text{f,liquid}}]_{\vartheta_{\text{in}}}^{\vartheta_{\text{evaporation}}}(\vartheta_{\text{evaporation}} - \vartheta_{\text{in}}) + r + ([c_{p,\text{f,gas}}]_{\vartheta_{\text{evaporation}}}^{\vartheta_{\text{out}}}(\vartheta_{\text{out}} - \vartheta_{\text{evaporation}}))) \tag{7}$$

In further discussion, the heat release and balance heat supply are referred to the volume of the evaporator *V*. With

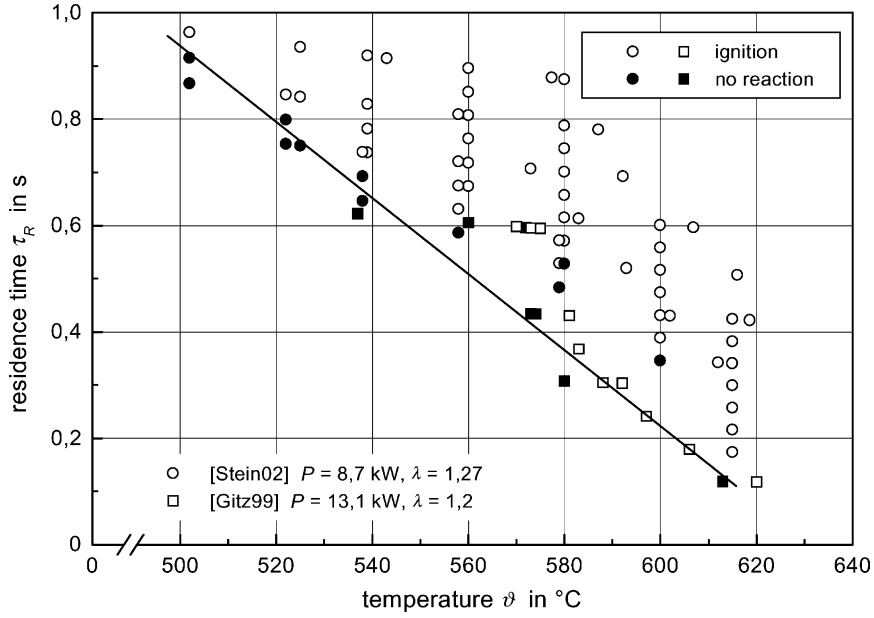

Fig. 2. Thermal ignition of IGO/air mixture in a flow reactor in respect to the residence time τ_{R} and temperature ϑ, $p = 1$ bar [2,3].

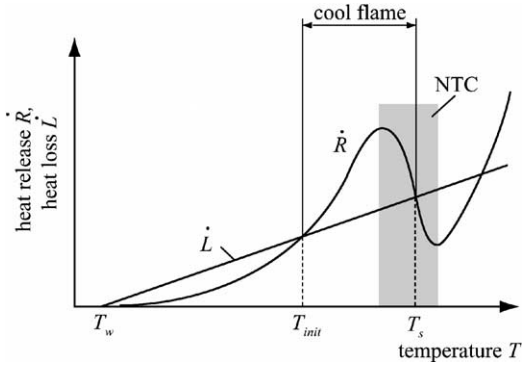

Fig. 3. Relationship between the heat release and the heat loss rate in a closed vessel at different fixed surface temperatures for a mixture with NTC characteristic.

this notation, the values can be directly referred to Eqs. (1) and (2). Whereas, $\dot{B}$ means the negative of the heat losses $\dot{L}$.

$$\dot{R} = \frac{\dot{Q}_r}{V} \tag{8}$$

$$\dot{B} = \frac{\dot{Q}}{V} = -\dot{L} \tag{9}$$

2.2. Diesel reformer

The diesel reformer is designed to produce fuel cell suitable gases under atmospheric pressure by partial oxidation or autothermal reforming. The kind of reforming process, e.g. catalytic or thermal is directly related to the sulphur content of the liquid fuel. If marketable IGO is the fuel, the fuel processor has to work at high temperatures without catalysts so that sulphur components in the fuel do not lead to a degradation of the system. If diesel fuels with sulphur contents below 50 ppm are involved, catalytic fuel processing is the choice (Fig. 5).

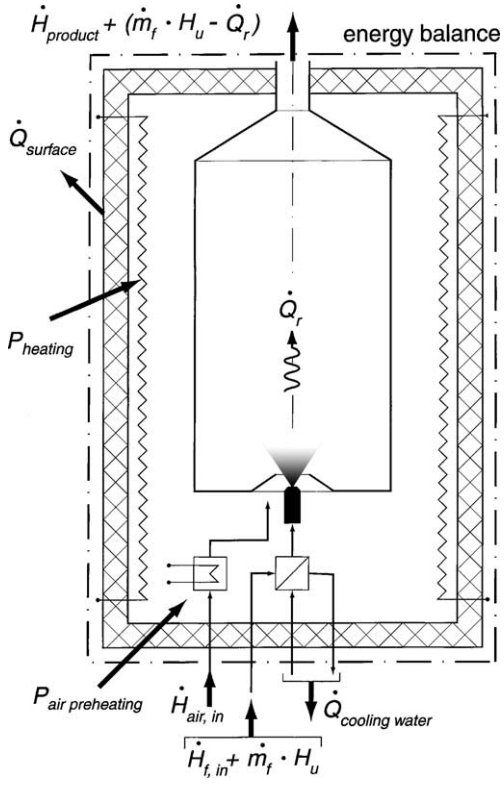

Fig. 4. Heat fluxes and flows of enthalpy of the evaporator tube [1].

The reformer consists of two process stages, the evaporator and the catalytic-reforming zone. In case of thermal partial oxidation, a ceramic porous matrix is used to stabilize the reaction zone. The homogeneous mixture of the liquid fuel and the air is produced in the first reaction chamber using exothermic cool flame pre-reactions. With a temperature of 400–480 °C, the mixture is transferred into the second stage of the fuel processor to be converted by thermal

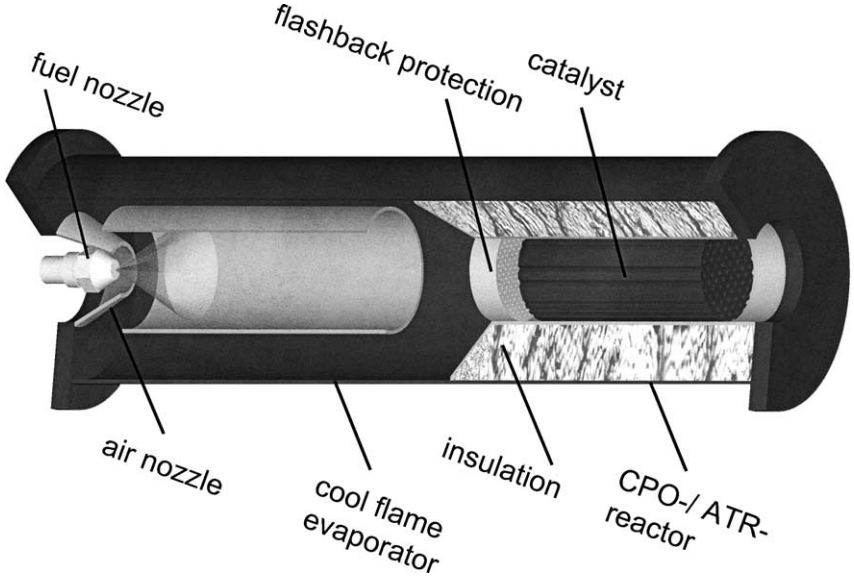

Fig. 5. Catalytic diesel reformer.

or catalytic partial oxidation or by autothermal reforming if water vapour is supplied. A flashback protection is implemented to decouple both reaction chambers thermally as well as to prevent flash back.

3. Results and discussion

3.1. Mixture preparation by cool flames

As can be seen in Fig. 3, the stable temperature T_s of the cool flames reaction can be characterised by the heat losses of the system. Beyond this, further influences exist for the ratios of fuel, air and inert gases. The influence of air ratio and air inertisation on the cool flame temperature is given in Fig. 6. In technical reformers, inertisation can result from fuel cell anode gas or water vapour to control the partial oxidation temperature. Under the chosen boundaries, the inertisation results from substitution of the air by combustion products. The ratio of the mass flows of inertisation gas to air is defined as the recirculation ratio r.

$$r = \frac{\dot{m}_{\text{inert}}}{\dot{m}_{\text{air}}} \tag{10}$$

The inlet temperature is independent from the recirculation rate constant at 400 °C. The wall temperatures are adjusted in the same magnitude. Without admixture of combustion products, the cool flame temperature increases proportional to decrease in the air ratio, λ. Under the chosen boundary, air ratios below $\lambda = 0.68$ led to auto-ignition of the mixture. By increasing inertisation, the cool flame temperature reduces significantly so that auto-ignition can be inhibited. The linear relationship between the cool flame temperature and the air ratio lasts in spite of the inertisation.

At air ratios below $\lambda = 0.2$, the linear coherence between the cool flame temperature and the air ratio is not remarkable anymore (Fig. 7). Instead of that, at $\lambda = 0.15$, the cool flame temperature reaches a maximum which is followed by a temperature decrease with lower air ratios. In this case, the lack of oxygen limits the cool flame reaction conversion.

Although the temperatures of the cool flame and the partial oxidation approach at low air ratios a general difference can be deduced from the temperature courses. With the exception of air ratios below $\lambda = 0.2$, the cool flame decreases with rising air ratio whereas the adiabatic POX temperature increases. This is caused by the fact that higher air ratios mean a higher heat capacity which has to be heated up by the cool flame reaction. However, the conversion is limited both by the oxygen fraction and by the partial pressure of the hydrocarbons.

In Fig. 8, the adjustable ranges of the cool flames are drawn in respect to the air ratio λ and the volume-based balance heat supply $\dot{B}$ of the system for $P = 5$ and 9 kW.

The ranges of high-temperature oxidation as well as the regions where no reaction can be observed shift with higher heat supply $\dot{B}$ to increasing air ratios. Lower air ratios prevent reaction quenching. Crucial is the lower heat capacity to heat up which causes higher reaction temperatures of the cool flame. The same effects are responsible for auto-ignition at higher heat supplies. If so the heat release tops the heat loss which is transferred by the reactor wall and the enthalpy flow of the product gas.

The lower boundaries of stability (no reaction) for $P = 5$ and 9 kW are in the same magnitude. That implicates that the residence times, which change in the order of two, are negligible. However, the upper boundaries of stability (high-temperature oxidation) differ significantly. Higher power output facilitates supply of higher values of heat into

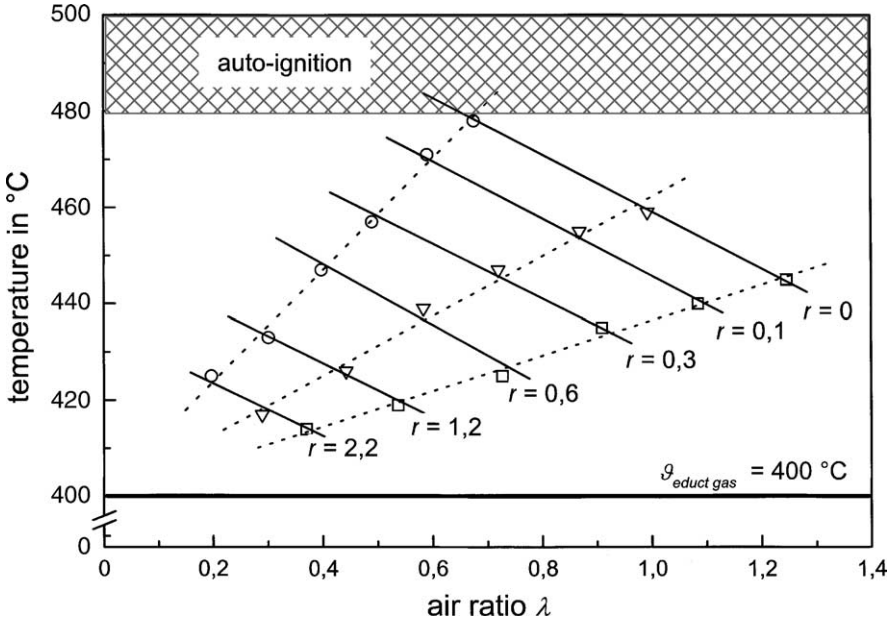

Fig. 6. Influence of air ratio λ and inertisation on cool flame temperature ($d = 100$ mm, isothermal conditions, IGO) [1].

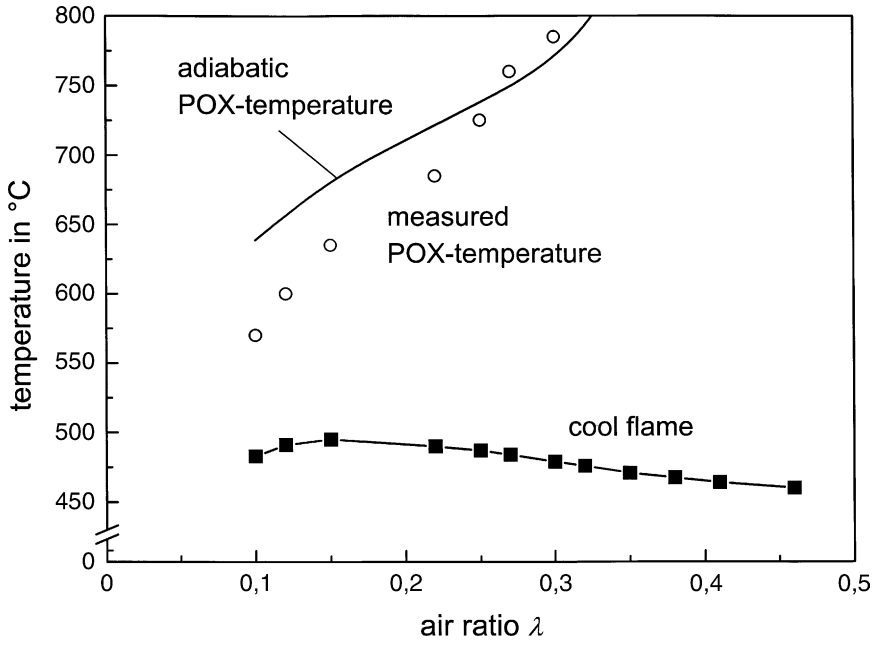

Fig. 7. Influence of air ratio λ and inertisation on cool flame temperature ($d = 100$ mm) [1].

the evaporator since the specific heat supply and the residence times decrease. It can be recognised that the evaporator runs autothermal up to air ratios $\lambda = 0.35$. So no heat transfer from the high-temperature zone of the reformer is needed for the cool flame operation.

The measured heat release $\dot{R}$ of the cool flame reaction for $P = 5$ kW calculated by Eqs. (4)–(8) is drawn in Fig. 9. The heat release increases proportional with the air ratio due to the fact that the gas temperature only changes a little. On the other hand, the heat capacity rises with higher values of the air ratio. The heat release rises with higher heat losses since the cool flame temperature remains almost on the same level. Independent from the value of heat supply/losses, the slope of the curves is nearly the same. Compared to the fuel input, up to 10% of the calorific value can be converted into heat by cool flame reactions.

3.2. Calculated reforming efficiency

Generally, two basic processes of fuel reforming are differed in the state-of-the-art. Steam reforming is strongly endothermic whereas partial oxidation is exothermal. The

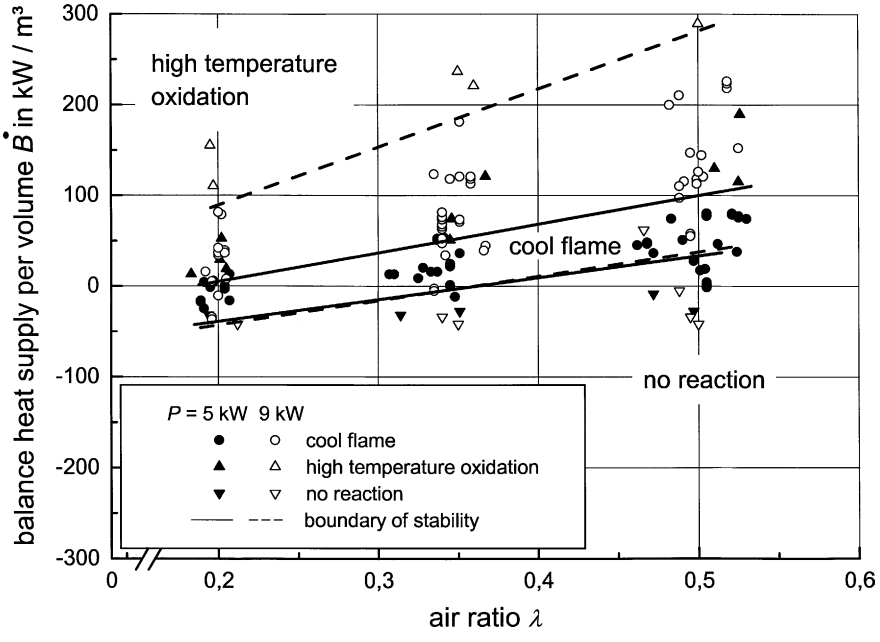

Fig. 8. Cool flame boundaries in respect to the heat supply/loss $\dot{B}$ and air ratio λ ($d = 70$ mm) [1].

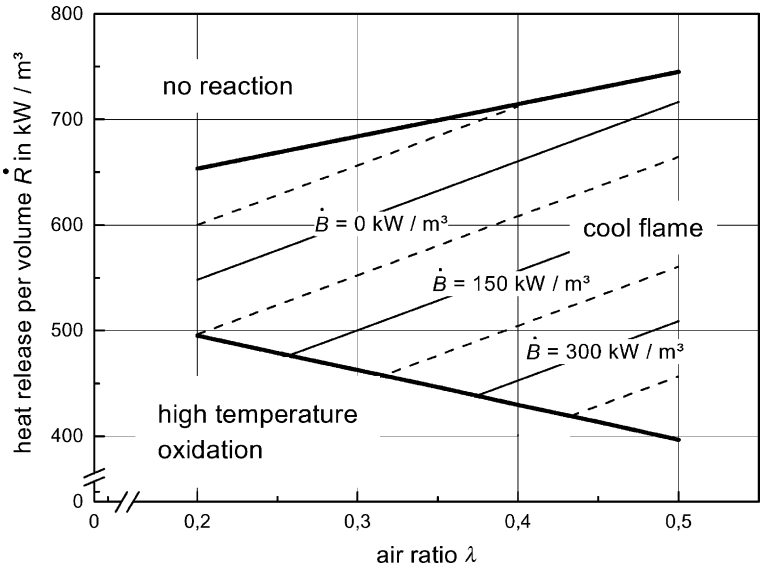

Fig. 9. Heat release of the cool flame reaction in respect to heat supply/loss $\dot{B}$ and air ratio λ ($d = 70$ mm, $P = 5$ kW) [1].

autothermal reforming can be classified between both methods. In all, described processes the hydrocarbon reforms catalytically at around 800 °C to form hydrogen and carbon monoxide. The reforming efficiency is a quantitative value that gives information about the energy content of the product gas after fuel processing. In this paper, the reforming efficiency η_{ref} is defined as the ratio of the heating value of product gas to fuel (Eq. (11)). The data for the fuel $H_{u,f}$ and hydrogen H_{m,H_2} are based on the lower heating value (LHV).

$$\eta_{ref} = \frac{(\dot{n}_{H_2} + \dot{n}_{CO})H_{m,H_2}}{\dot{m}_f H_u} \quad (11)$$

The quantities for hydrogen and carbon monoxide have been calculated by thermo-chemical equilibrium by minimising the Gibbs' enthalpy using the Chemkin database. With a fixed reforming temperature of 800 °C the reforming efficiency for diesel is given as a function of the air ratio λ and the steam-to-carbon ratio, SCR, in Fig. 10. Reforming temperatures below 750 °C lead to undesirable formation of hydrocarbons and soot. The heat that has to be supplied or discharged of the process is drawn in Fig. 11.

Generally, the reforming efficiency increases with decreasing air ratios while sufficient water takes place in

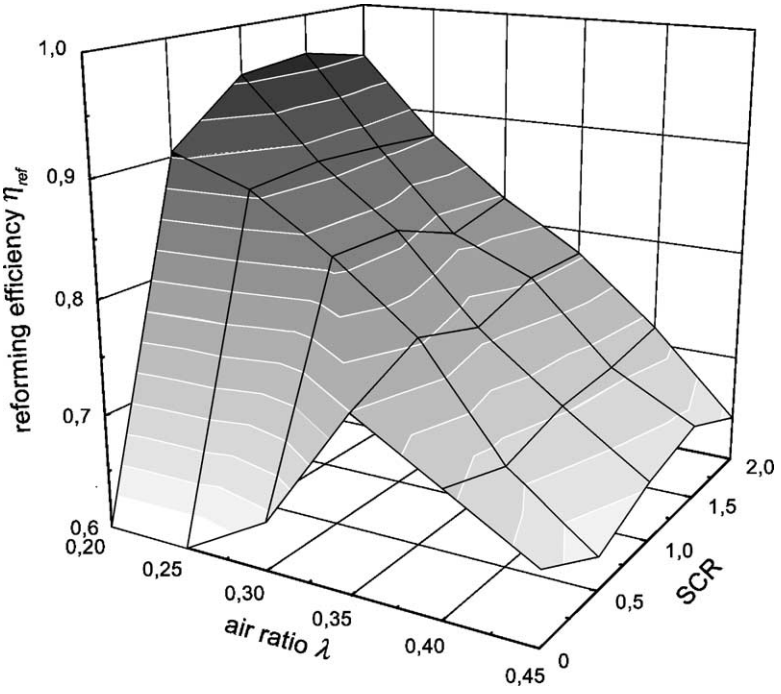

Fig. 10. Reforming efficiency η_{ref} for isothermal diesel reforming at 800 °C [4].

the reforming reaction. For pure partial oxidation without water vapour reforming efficiencies of $\eta_{ref} = 0.75$ can be expected for $\lambda = 0.35$. Through water supply this value can be raised. Autothermal conditions are reached when the specific heat flux has negligible amounts for example for $\lambda = 0.35$ and SCR = 0.4. In these operation points, about 82% of the fuel calorific value remains in the product gas.

3.3. Thermal partial oxidation

Among catalytic-reforming processes, thermal partial oxidation (TPOX) of IGO had been examined. The measured gas concentrations are given in Fig. 12. Compared to catalytic-reforming processes, TPOX is non-sensitive to fuel impurities like sulphur components. In this case, a hot gas desulphurisation after TPOX is sufficient for sulphur purification.

It can be seen that the reforming temperature has a crucial effect on the hydrogen yield. For the hydrogen production, the influence of the reaction temperature is more important than the air ratio. Temperatures above 1200 °C are necessary to achieve a satisfying hydrocarbon conversion. Therefore, air ratios about $\lambda = 0.45$ and higher has to be adjusted. Especially minimised heat losses of the fuel processor are mandatory. Best reforming efficiencies of $\eta_{ref} = 0.70$ has been reached at $\lambda = 0.46$.

3.4. Catalytic partial oxidation

The motivation to involve catalytic processes for reforming is to lower the process temperature, which is necessary to reach equilibrium concentration as well as the volume, which is needed for a complete conversion. Compared to the above mentioned TPOX, a reduction in volume by factor of 20 of the reformer reactor can be achieved in our case. At the same time, the process temperature can be decreased at least by 200–300 K. This leads directly to fewer requirements of materials, lower heat losses and a decrease in the thermal response time. The fuel used in all catalytic processes is an alkane-rich fuel with sulphur content below 10 ppm. The fuel properties are given in the Appendix A of this paper. The influence of the catalyst volume (expressed by the space velocity, SV) on the product yield is given in Fig. 13.

The boiling range is comparable to diesel and IGO. Already space velocities more than SV = 40,000 h^{-1} are sufficient for main hydrocarbon conversion. A decrease in the product yield at space velocities below SV = 20,000 h^{-1} is due to an increase of the reforming temperature which causes a shift in the thermo-chemical equilibrium.

If the air pre-heating temperature is below the initialisation temperature of the cool flame, about 300 °C an evaporation operation without cool flames can be realised. Fig. 14 gives a comparison of both operation modes. Without cool flames, an evaporation temperature about 180 °C results with an air pre-heating temperature of 250 °C. With cool flames the evaporation temperature reaches 410 °C. As a result from the advanced mixture preparation by cool flames, the inlet temperature of the CPO catalyst decreases by 50 K. Another imaginable reason for the decrease of the inlet CPO temperature can be attributed to the hydrocarbon conversion by cool flames. Among other reactions, the formation of water in the cool flame reaction can be significant by the following mechanism:

alkane + oxygen → olefin + water

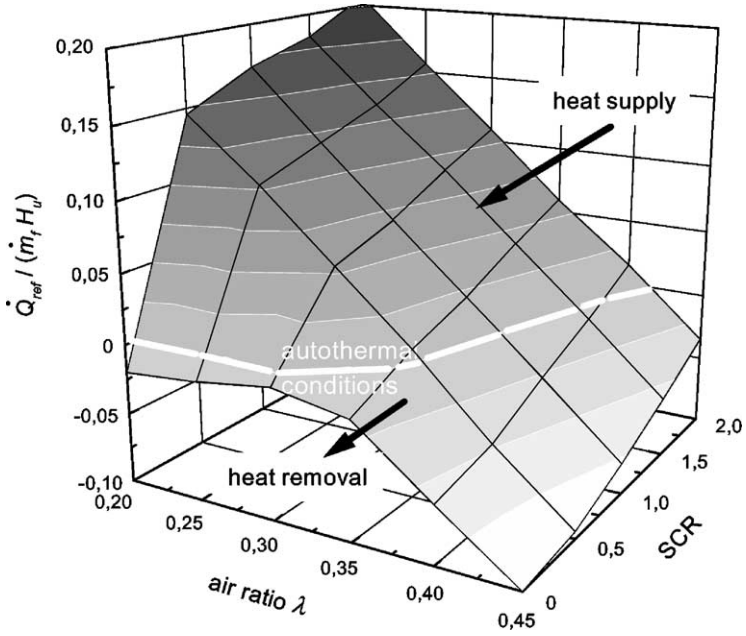

Fig. 11. Reforming heat based on fuel power $\dot{Q}_{ref}/(\dot{m}_f H_{u,f})$ for isothermal diesel reforming at 800 °C (ϑ_{educts} = 25 °C) [1].

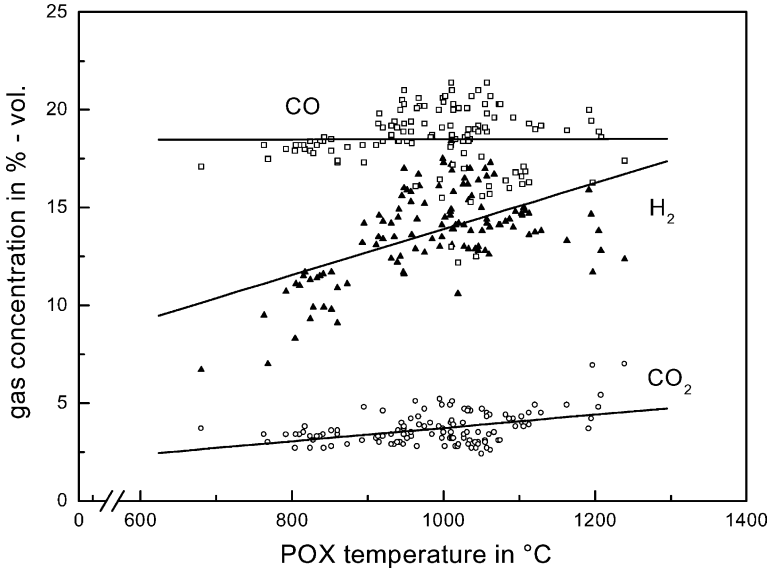

Fig. 12. Gas concentrations in respect to the reforming temperature for thermal partial oxidation of IGO ($\lambda = 0.40$–0.46, $\vartheta_{air} = 250$ °C, $P = 4.7$–7.2 kW) [1].

Measurements of cool flames products for *n*-heptane verify olefin yields about 10% [5]. The dominant cooling effect is that endothermic steam-reforming reactions already occur simultaneous in the catalyst entry. This is facilitated by the existence of water formed by cool flames. Furthermore, the reforming efficiency increases by the advanced evaporation by cool flames from $\eta_{ref} = 0.67$ to 0.74.

Fig. 15 gives the gas concentrations, the reforming temperature and reforming efficiency for CPO in respect to the air ratio λ. In comparison with the calculated data in Fig. 10, the reforming efficiency rises with higher air ratios up to $\lambda = 0.39$. Similar to the results of TPOX, a slight relationship between the reforming efficiency and the reforming temperature can be observed.

The measured inlet temperatures of the CPO catalyst between 950 and 1000 °C exceed the operation temperature of the reforming catalyst which is limited by 900 °C. A degradation of the catalyst cannot be avoided. On the other hand, if the air ratio is reduced, the formation of soot can be predicted by thermo-chemical calculations.

As can be seen in Fig. 16, a narrow sector remains for CPO operation. Under real conditions, the CPO temperature exceeds the adiabatic temperature because of the slow kinetics of the reforming reaction in comparison with the oxidation reactions.

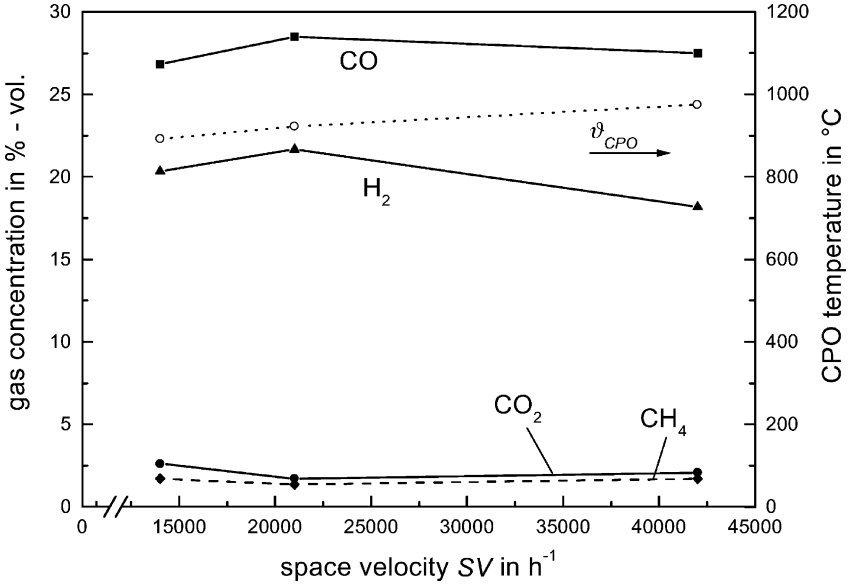

Fig. 13. Gas concentrations and reforming temperature in respect to the space velocity, SV, for catalytic partial oxidation of sulphur-reduced diesel ($\lambda = 0.36$, $P = 5.8$ kW, $\vartheta_{air} = 250$ °C) [1].

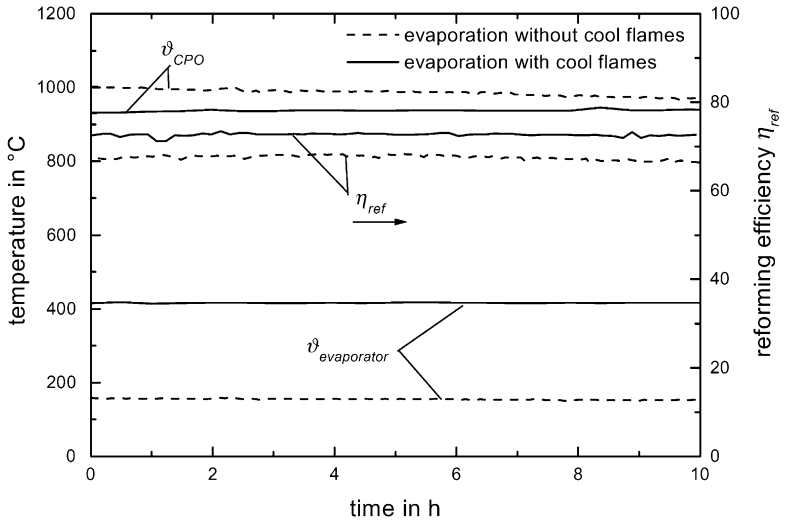

Fig. 14. Gas concentrations, the reforming temperature and reforming efficiency for CPO in respect to the air ratio λ for catalytic partial oxidation of sulphur-reduced diesel ($\lambda = 0.36$, $P = 5.8$ kW, $\vartheta_{air} = 250$ °C, SV = 21,000 h^{-1}) [4].

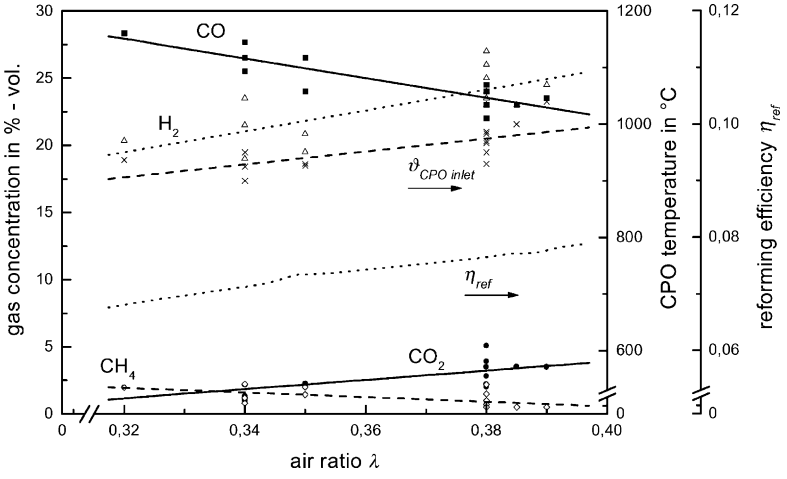

Fig. 15. Gas concentrations, reforming temperature and reforming efficiency for CPO in respect to the air ratio λ for CPO of sulphur-reduced diesel ($\lambda = 0.36$, $P = 5.8$ kW, SV = 21,000 h^{-1}, $\vartheta_{air} = 250$ °C) [1].

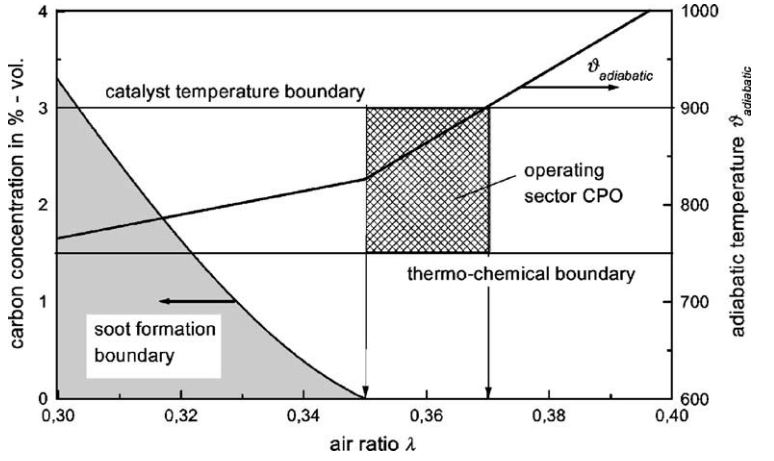

Fig. 16. Operation sector for CPO of diesel/IGO [1].

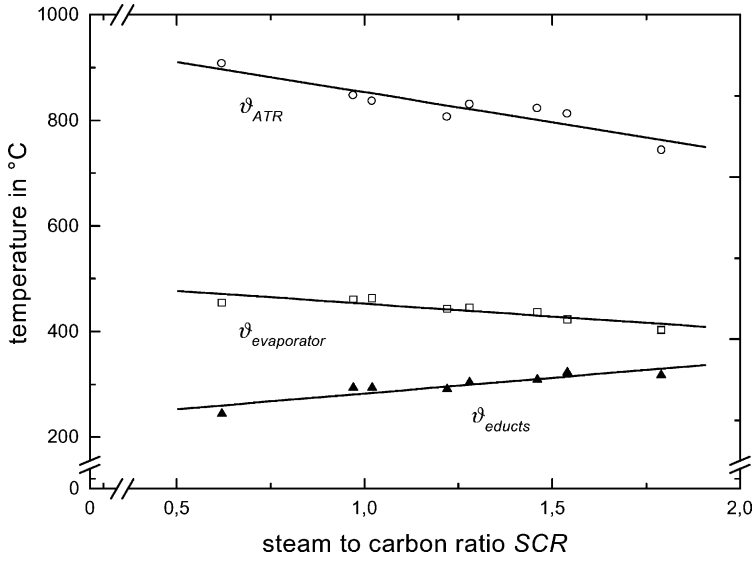

Fig. 17. Measured temperatures in the ATR reformer in respect to SCR, sulphur-reduced diesel ($\lambda = 0.30$, $P = 5.8$ kW, SV = 30,000 h^{-1}) [1].

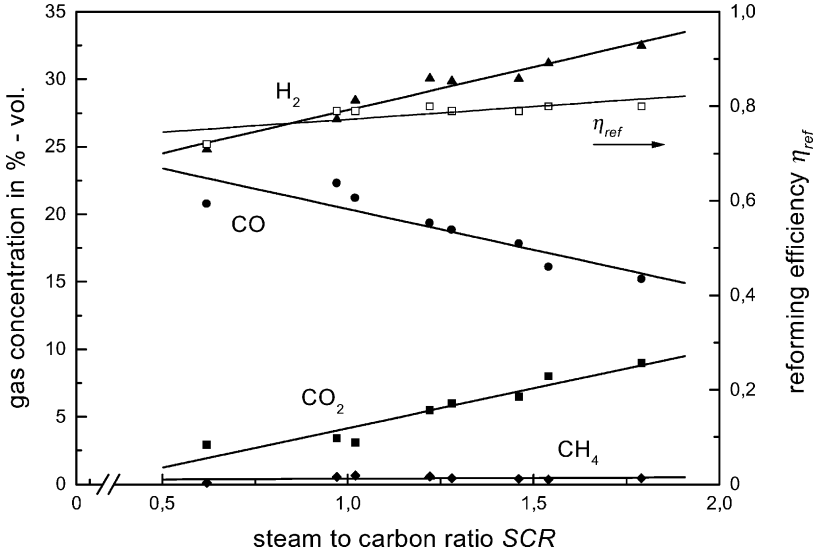

Fig. 18. Gas concentrations reforming efficiency for ATR in respect to SCR, sulphur-reduced diesel ($\lambda = 0.30$, $P = 5.8$ kW, SV = 30,000 h^{-1}) [1].

Extension of the operation sector for CPO is achievable by:

- optimisation of the catalyst performance by lifting the operation temperature;
- off-gas recirculation;
- water modulation.

Latter point means a shift from catalytic partial oxidation to autothermal reforming.

3.5. Autothermal reforming

By supply of water vapour the reforming temperatures can be controlled more easily. First, water vapour substitutes the amount of oxygen and allows lower air ratios than CPO. Second, water vapour provides endothermic reforming reactions. Within the examinations, water vapour is produced externally and is mixed with the combustion air before the air nozzle.

The measured temperatures for ATR operation in respect to the steam-to-carbon ratio, SCR, are given in Fig. 17. Both the temperatures in the cool flame evaporator and the ATR decrease with increasing SCR. Even at SCR = 0.5 the maximum operation temperature is reached in the shown measurements. Depending on the water input the cool flame reactions causes a temperature lift of up to 200 K.

The measured gas concentrations and heron calculated reforming efficiencies are given in Fig. 18. As expected, the hydrogen and carbon dioxide yields increase with higher water vapour supply, whereas the concentration of carbon monoxide decreases. The measured hydrocarbon concentration is strictly below 0.5%, independent of the value of SCR.

A degradation of the catalyst cannot be observed even under a 400 h operation.

Appendix A

Fuel properties of Shell Sol D100

Boiling range	235–270 °C
Calorific value (H_u)	45.2 MJ/kg
Carbon mass fraction	0.8522
Hydrogen mass fraction	0.1478
Sulphur content	<10 mg/kg
Alkane fraction	0.5
Naphthene fraction	0.5
Aromatic fraction	<2000 mg/kg

References

[1] L. Hartmann, Untersuchungen zu Kalten Flammen in der Unterstöchiometrie zur Realisierung eines Brennstoffzellenreformers für flüssige Brennstoffe, Ph.D. Thesis, RWTH Aachen, 2002.
[2] H.P. Gitzinger, Nutzung Kalter Flammen für die Gemischbildung zur Realisierung eines Strahlungs brenners für flüssige Brennstoffe, Ph.D. Thesis, RWTH Aachen, 1999.
[3] N. Steinbach, Untersuchungen zum Zündverhalten von Heizöl EL-Luft-Gemischen unter atmosphärischen Druck, Ph.D. Thesis, RWTH Aachen, 2002.
[4] L. Hartmann, K. Lucka, C. Mengel, H. Köhne, POX-reformer for gas oil/diesel in stationary and automotive SOFC-technologies, in: Proceedings of the 5th European Solid Oxide Fuel Cell Forum, vol. 2, Lucerne, 2002.
[5] C. Mengel, K. Lucka, H. Köhne, O. Hein, A. Jess, Umwandlung von leichtem Heizöl in ein homogenes Brenngas-Luftgemisch mittels Kalter Flammen, Erdgas, Erdöl, Kohle, 118. Jahrgang, Heft 10, Oktober 2002.